In-Depth Investigation of Protein Adsorption on Gold Surfaces: Correlating the Structure and Density to the Efficiency of the Sensing Layer

Souhir Boujday,*[,†,‡] Aurore Bantegnie,[†,‡] Elisabeth Briand,[†,‡] Pierre-Guy Marnet,[||] Michèle Salmain,[§] and Claire-Marie Pradier[†,‡]

UPMC Univ Paris 6, UMR CNRS 7609, Laboratoire de Réactivité de Surface, F75005 Paris, France, CNRS, UMR 7609, Laboratoire de Réactivité de Surface, F75005 Paris, France, Laboratoire de Chimie et Biochimie des Complexes Moléculaires, UMR CNRS 7576, Ecole Nationale Supérieure de Chimie de Paris, F75005 Paris, France, and Agrocampus-Rennes, Département des sciences animales, UMR ENSAR/INRA, 35042 Rennes, France

Received: December 19, 2007; Revised Manuscript Received: March 5, 2008

Protein A (PrA), mouse monoclonal anti-IgG antibody (SAb) and deglycosylated avidin (NAV) were adsorbed on gold surfaces to capture the model rabbit IgG and build three immunosensing platforms. The assembling of immunosensors, their specificity, and the receptor accessibility were monitored by polarization modulation reflection–absorption infrared spectroscopy (PM-RAIRS) and quartz crystal microbalance with dissipation measurement (QCM-D) at each step. Combining these two techniques allows us to compare both chemical and structural properties of the sensing layers with the former bringing chemical and semiquantitative information on the grafted protein layers, whereas the latter, in addition to the mass uptake, enables us to take the layer rigidity into account. Grafting of the three capture proteins to the transducer surfaces, covered with appropriate self-assembled monolayers, yielded protein layers with variable properties. NAV formed a dense and rigid molecular layer, likely containing protein aggregates, whereas the amount of PrA was below one monolayer resulting in a flexible layer. The amount of immobilized rabbit IgG was different for the three systems with the densest capture protein layer exhibiting the lowest binding capacity. The accessibility of antibodies on the resulting immunosensors measured by interaction with a secondary antirabbit IgG antibody was found to be closely dependent on their coverage as well as on the rigidity of the protein layer. The overall study provides in-depth information on three of the most common immunosensor recognition interfaces and demonstrates the crucial influence of both structure and density of the protein layer on the efficiency of the molecular recognition phenomena.

Introduction

Immunosensors currently appear as one of the fastest growing technologies because of their unique ability to detect and quantify biological or nonbiological targets like proteins, toxins, or pollutants with extreme sensitivity and specificity.[1] Once the difficulty of generating specific antibodies for the target is overcome, the key point is the choice of the antibody immobilization method used to create the biorecognition interface as it should ensure the optimal orientation but also high density and accessibility of the antibody binding sites.[2,3]

Among the wide variety of reported methods for grafting antibodies to gold transducers, including physical or chemical adsorption, we focused the present work on those based on their immobilization by means of three capture proteins, chemically grafted on a self-assembled monolayer (SAM). To the best of our knowledge, there have been very few systematic comparisons of antibody immobilization methods using bioaffinity associations.[4] Moreover, the influence of factors like receptor coverage and accessibility or sensing layer flexibility on the efficiency of the molecular recognition process is rarely investigated, and this will be the topic of the present work.

Protein A (PrA), avidin in its deglycosylated form (NAV), and a monoclonal antirabbit IgG secondary antibody (SAb) were selected for this study because of their high affinity for rabbit IgG (rIgG) or its biotinylated derivative. For the three systems, the density and the accessibility of antibodies, as well as the specificity of the resulting sensing layers, were characterized and compared to each other.

PrA, a cell wall protein of *Staphylococcus aureus* is known to bind to the Fc part of IgG-type antibodies of various species.[5] Using PrA as a binding protein is a well-known way to orient IgG molecules with respect to the transducer surface;[6] this method has been described and compared to other nonoriented immobilization procedures in refs 7 and 8 and references therein. Although the biosensor properties were similar, the PrA immobilization method is favored because of better stability and reproducibility of the IgG layer, as compared to covalent binding methods. Most of the time, PrA is grafted on the gold transducer surface via chemisorbed SAMs.[9,10]

The specific and high affinity biotin–avidin association has been used for quite a long time in numerous immunoassays;[11–14] it requires the preparation of biotinylated derivatives, for example, enzymes[15,16] or antibodies, which of course constitutes a time-consuming additional step. However, once the biotinylated molecule is prepared, this type of process, due to the high affinity constant, guarantees a very easy and stable immobilization.

Eventually, the SAb used in the present study is a mouse monoclonal antirabbit IgG antibody directed against the Fc part

* To whom correspondence should be addressed. Tel: +33144276001. Fax: +33144276033. E-mail: souhir.boujday@upmc.fr.
† UPMC Univ Paris 6, UMR CNRS 7609.
‡ CNRS, UMR 7609.
|| UMR ENSAR/INRA.
§ Ecole Nationale Supérieure de Chimie de Paris.

10.1021/jp711916g CCC: $40.75
Published on Web 05/07/2008

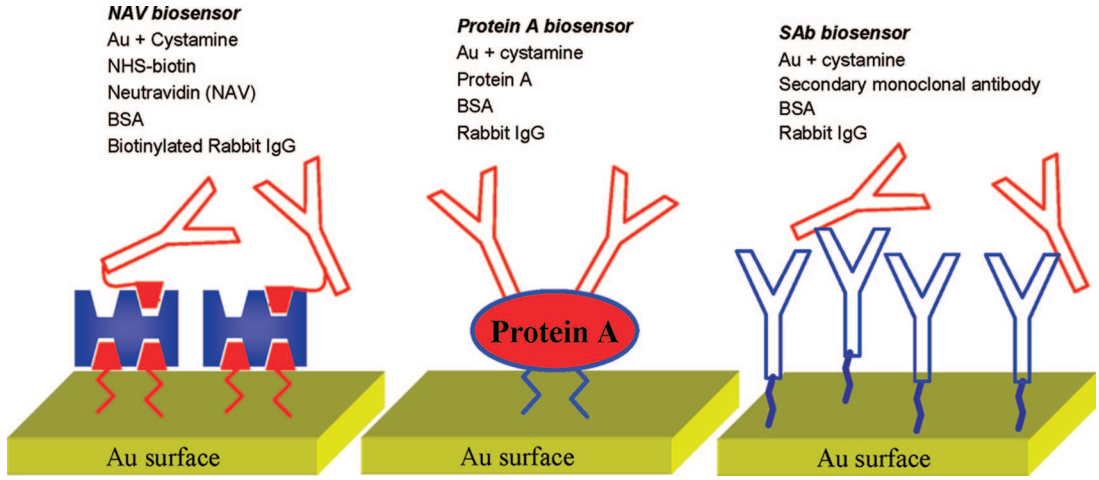

Figure 1. Investigated affinity binding systems.

of rIgGs; it will strongly bind to rIgG type antibodies also allowing them to be oriented with respect to the solid surface. Working with a secondary antibody that captures the primary antitarget antibody, though often used in classical solid-phase immunoassays, is a rather novel approach for immunosensor development.[17,18] It is interesting to prepare a dense layer of secondary anti-rIgG antibodies and characterize their ability to bind rIgG in an efficient way, compared to the two previous methods. Using PrA or SAb seems to constitute rather similar principles of immobilization but so far for an unclear reason only the former has been used to construct immunosensors. It is worth comparing them for the same receptor: a model rIgG.

The three affinity proteins, NAV (via biotin), PrA, and SAb, were covalently immobilized to the transducer's surface starting from the same NH_2-terminated SAM, according to the schemes shown in Figure 1. Then, the model rIgG was immobilized by affinity to the protein layers, and the amount of bound antibodies and their accessibility, evaluated by the binding of a goat anti-rIgG antibody, were compared.

Polarization modulated-reflection–absorption infrared spectroscopy (PM-RAIRS) and quartz crystal microbalance with dissipation (QCM-D) were used to characterize the adsorption phenomena at each step of the immunosensors' elaboration as well as to assess the amount of bound rIgG molecules and determine their accessibility. These two techniques provide complementary information. PM-RAIRS provides chemical semiquantitative characterization of the molecular layers once they have been deposited. QCM-D allows real-time measurement of protein adsorption at the solid–liquid interface and, when the resulting layer is rigid, the resonant frequency variation ΔF is proportional to the mass uptake.[19] Simultaneous access to energy dissipation ΔD provides useful information on the layer structure and viscoelasticity. This will be discussed in the light of the data measured on the three elaborated sensing systems. The aim of our contribution is 2-fold, (1) comparing three methods for the immobilization of antibodies leading to three sensing layers differing in their structure, density of receptor, and viscoelastic properties and, (2) discussing all the information brought by complementary surface characterization techniques to understand how the layer structure may influence the amount of immobilized antibodies and their accessibility.

Experimental Section

Material and Procedures. ***Amine-Terminated SAM Assembling.*** IR and QCM sensors were immersed in 10 mL of a 10^{-2} M aqueous solution of cystamine (Aldrich) during 12 h. Finally, substrates were rinsed in the same volume of ultra pure water and dried under nitrogen flow.

NAV Immunosensor Elaboration. Amine-terminated IR and QCM sensors were immersed in a 10^{-2} M Biotin-NHS (Aldrich) solution in dimethylformamide (DMF). This experiment was carried out in a glovebag under nitrogen. After 12 h, substrates were washed twice in DMF and a third time in ethanol. Then substrates were treated by a 0.1 mg/mL solution of neutravidin (Pierce) in phosphate-buffered saline (PBS) buffer (pH = 7.4) during 2 h. After three washing in PBS, substrates were treated by a 0.1 mg/mL solution of BSA (Aldrich) in PBS for 30 min and then washed three times in PBS. Finally, the sensors were exposed to a 0.1 mg/mL solution of biotin-SP rabbit IgG (Fluoroprobes). After 1 h, samples were rinsed twice in PBS, a third time in ultrapure water, and then the IR sensors were dried under nitrogen flow.

PrA Immunosensor Elaboration. Amine-terminated IR and QCM sensors were treated by a 0.1 M solution of glutaraldehyde in EtOH for 12 h. They were extensively rinsed with EtOH then immersed in a 0.1 mg/mL solution of recombinant Protein A (Pierce) in PBS. After 2 h, substrates were washed three times with PBS, then in a 0.1 mg/mL solution of BSA (Aldrich) in PBS for 30 min, and then washed again three times in PBS. Finally, the sensors were exposed to a 0.1 mg/mL solution of rabbit IgG (Aldrich) in PBS. After 1 h, the samples were rinsed twice in PBS, a third time in ultrapure water, and then the IR sensors were dried under nitrogen flow.

Secondary Antibody (SAb) Immunosensor Elaboration. The carbohydrate residues of the antibody were first oxidized following a procedure adapted from ref 20. Sodium metaperiodate (50 mM in 0.1 M acetate buffer, pH = 5.5) was added to a solution (0.5 mL, 1 mg/mL) of monoclonal mouse antibody against the Fc fragment of rabbit IgG, provided by Pr. Pierre-Guy Marnet (Agrocampus-Rennes, Département des sciences animales, UMR ENSAR/INRA). After 20 min, the oxidized antibody was purified by gel filtration using a prepacked 5 mL gel desalting column (Pierce) with 50 mM sodium phosphate buffer pH 8 as eluent. The sensors were exposed to the solution of oxidized SAb and after 1 h to a 50 mM solution of $NaCNBH_3$ in the same buffer to reduce the imine functions. Finally, residual aldehydes were blocked by treating the sensors with 1 M ethanolamine pH 9.0. BSA and rabbit IgG were then deposited on the surface following the same conditions as for PrA immunosensor, which was described above.

Immunosensors Selectivity and Receptors Accessibility. The accessibility of the rIgG receptors was investigated by spotting

150 μl of a 0.1 mg/mL solution of goat antirabbit IgG (Aldrich) in PBS on the immunosensor surface. On QCM sensors, this was studied by injecting 4 mL of the same antigen solution. After 1 h, QCM sensors were rinsed three times in PBS solution. IR sensors were rinsed once followed by 2 ultrapure water washes before PM-RAIRS experiment. Immunosensors selectivity was investigated with a 0.1 mg/mL solution of goat serum proteins (Aldrich) in PBS. The experimental conditions of incubation and washing steps were the same as those used for anti-rIgG immobilization.

PM-RAIRS. PM-RAIRS spectra were recorded on a commercial NICOLET Nexus spectrometer. The external beam was focused on the sample with a mirror at an optimal incident angle of 75°. A ZnSe grid polarizer and a ZnSe photoelastic modulator, modulating the incident beam between p and s polarizations (HINDS Instruments, PEM 90, modulation frequency = 37 kHz), were placed prior to the sample. The light reflected at the sample was then focused on a nitrogen-cooled MCT detector. The presented spectra result from the sum of 124 scans recorded with 8 cm^{-1} resolution. The PM-IRRAS signal is given by the differential reflectivity $\Delta R/R = (R_p - R_s)/(R_p + R_s)$. IR sensors were glass substrates (11 × 11 mm) successively coated with a 50 nm thick layer of chromium and a 200 nm thick layer of gold. These substrates were purchased from Arrandee (Werther, Germany). Before use, they were annealed in a flame, then rinsed in ultrapure water and dried under nitrogen flow.

QCM Measurements. Quantitative studies of molecules adsorption on gold surface during biosensors synthesis and reactivity were performed using a dissipative QCM (QCM-Z500, KSV Instruments, Finland). Experiments were carried on AT-cut planar gold electrode-coated quartz crystals (QCM sensors, 14 mm diameter) with a 5 MHz nominal resonance frequency (QuartzPro, Sweden). The measurement temperature was fixed at 25 °C using a thermal electric controller (Oven Industries-,Inc.). Before use, quartz crystal electrodes were cleaned by ethanol and dried under nitrogen flow. Data was simultaneously acquired at the fundamental frequency of 5 MHz ($N = 1$) and several overtone frequencies (15, 25, 35, 45, and 55 MHz). Two physical parameters are discussed: the frequency of oscillation and the dissipation. The frequency change can be correlated to the mass of the adsorbed layer using the Sauerbrey equation[19]

$$\Delta F = -N\Delta m/C_f$$

where C_f (=17.7 ng/cm^2·Hz at $f = 5$ MHz) is the mass-sensitivity constant, and N (=1, 3, 5, . . .) is the overtone number.

However, this equation is valid only if the added layer on the crystal surface is rigid. The rigidity of the layer is estimated thanks to the change in dissipation defined by

$$\Delta D = E_{dissipated}/2\Pi E_{stored}$$

where $E_{dissipated}$ and E_{stored} are the dissipated and stored energy during one oscillation.

In this paper, the presented frequency change (ΔF) and dissipation change (ΔD) are those measured at the third overtone ($N = 3$; $F = 15$ MHz).

Results

All immunosensors were constructed from a common thiolate SAM terminated by a primary amine group. This SAM was formed by chemisorption of cystamine under previously optimized conditions.[21] Protein molecular weights[5,18,22–25] and their estimated sizes[25–29] are summarized in Table 1 together with the resulting theoretical surface coverage $\Gamma_{(th)}$ required to form a full monolayer of each protein. PrA, NAV and the mouse anti-rIgG SAb were bound to the surface using various chemical strategies. PrA was covalently linked to the SAM by cross-linking with glutaraldehyde to couple the protein via its lysine residues.[30] SAb was site-specifically coupled by reductive amination to the cystamine SAM after oxidation of its carbohydrate residues into aldehydes.[20] As the carbohydrate residues of SAb are away from its antigen binding sites, this procedure may ensure a control of its orientation with respect to the surface. Eventually, NAV was immobilized by affinity to biotin covalently coupled to the aminated SAM by amide linkage.[31] These binding steps were followed by a treatment of the modified surfaces with a solution of BSA to avoid nonspecific antibody or antigen further adsorption. Finally, the antibody receptor, for example, rabbit IgG, was immobilized onto these three affinity platforms. Here again, for the NAV system, antibody immobilization was based on biotin/avidin affinity using biotinylated rIgG. These successive elaboration steps were investigated ex situ after rinsing and drying by PM-RAIRS and in situ by QCM-D.

TABLE 1: Structural Properties of the Proteins

	molecular mass (Da)[a]	approx surface (nm^2)[b]	$\Gamma_{(th)}$ (pmol cm^{-2})
NAV	60000	33	5.0
PrA	44600	20	8.3
BSA	66400	56	3.0
IgG (rIgG, anti-rIgG, or SAb)	150000	(67–140)[c]	2.5–1.2

[a] From refs 5, 18, and 23–25. [b] From refs 25–29. [c] Depending on the orientation of IgG.[25]

Immunosensor Elaboration Investigated by PM-RAIRS and QCM. PM-RAIRS spectra, recorded after the successive steps of immunosensor elaboration, are shown in Figure 2I. On all these spectra, one observes intense bands at 1655 cm^{-1} (amide I) and 1550 cm^{-1} (amide II). Their presence and intensity are directly correlated to protein adsorption. We previously showed that integrating amide band areas does provide direct semiquantitative information on the relative masses of adsorbed proteins.[3] Dividing these relative masses by the corresponding molecular weights provides information on the relative molecular amount of each protein. Figure 2II shows both relative mass and molecular amount data for the three capture proteins.

In situ frequency shifts measured by QCM-D were also recorded during the successive steps of immobilization on piezoelectric quartz crystals (Figure 3). The different steps are indicated by arrows on the graphs. The corresponding frequency shifts, dissipation values, and mass changes, measured at equilibrium, are summarized in Table 2. The frequency change ΔF versus time plot for the SAb system was quite complex due to changes of solvents during protein deposition (see Experimental Section). To minimize measurement errors, frequency changes were taken after the rinsing step, back to PBS. For the three sensing layers, quantitative QCM-D data will be considered with special attention and correlated to PM-RAIRS data to state on the possible role of the layer structure and rigidity on frequency changes. We do not exclude that water trapped in the protein layers and/or complex viscoelastic effects may induce an overestimation of the calculated masses;[27,32–34] however, one may assume similar error factors for the three capture proteins; the relative mass uptakes could thus be compared to each other. QCM frequencies presented hereafter will be correlated to mass uptakes in the first stages where dissipation is low.[35,36] Moreover, the normalized frequency

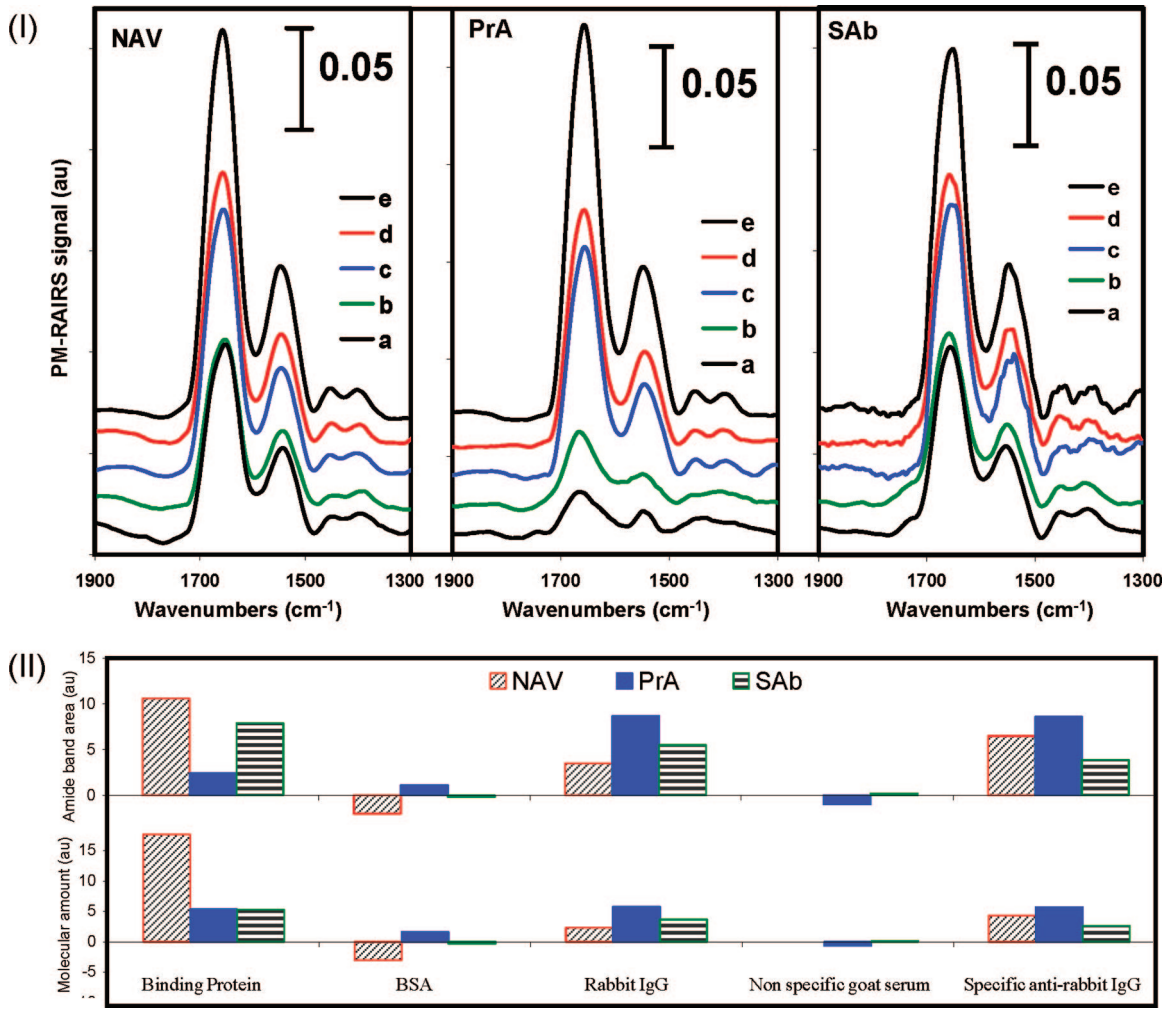

Figure 2. (I) PM-RAIRS spectra for the three systems NAV, PrA, and SAb during elaboration, specificity, and accessibility tests. (a) binding protein, (b) BSA, (c) rIgG, (d) goat serum, and (e) anti-rIgG. (II) PM-RAIRS data on the relative mass and molecular amount of adsorbed proteins during elaboration, specificity, and accessibility tests.

variation, Δf_n, where n is the harmonic number, was calculated for $n = 3$, 5, 7, and 9; its variations were small enough to confirm the absence of viscoelastic effect at that stage. At each step, the ratio $\Delta D/\Delta F$, whose increase indicates a more flexible layer,[37] will be evaluated and discussed.

Coupling of Affinity Proteins. The first PM-RAIRS spectra Figure 2Ia correspond to the binding protein deposition step. The integrated area of the amide I and II bands in Figure 2II was much lower for PrA than for the two other systems. However, dividing these integrated areas by the protein molecular weight yielded a molecular amount of PrA close to that of SAb and aproximately three times lower than that of NAV.

Adsorption of the three binding proteins was also monitored in situ by QCM-D (Figure 3). A significant decrease of the resonance frequency was observed when the piezoelectric sensors, modified by the cystamine SAM and activated by glutaraldehyde or biotin, were exposed to the solutions of binding protein. The frequency shifts measured at equilibrium are gathered in Table 2 together with the mass uptakes, Δm, calculated from the Sauerbrey equation[19] and estimated experimental surface coverages $\Gamma_{(ex)}$. The highest surface coverage was calculated for NAV (16.7 pmol cm^{-2}) followed by PrA (5.1 pmol cm^{-2}), and the lowest $\Gamma_{(ex)}$ was for SAb (2.7 pmol cm^{-2}). The amount of adsorbed NAV was very high in agreement with PM-RAIRS data, exceeding the theoretical monolayer surface coverage, $\Gamma_{(th)}$, estimated on the basis of the protein size (Table 1). The recorded dissipation change for this system is the highest one, but the $\Delta D/\Delta F$ ratio is close to that of SAb layer and lower than for PrA, which indicates a strong and compact film for both NAV and SAb systems. For protein A, a low amount is adsorbed, as previously suggested by PM-RAIRS, corresponding to approximately 60% of a full monolayer when $\Gamma_{(ex)}$ is compared to the theoretical coverage $\Gamma_{(th)}$ (Table 1). This low coverage may explain the high $\Delta D/\Delta F$ ratio that indicates a flexible protein layer. A good correlation between the PM-RAIRS and the QCM data was observed for PrA and NAV, giving a surface density ratio NAV/PrA close to 1.5. Eventually, for the SAb system the surface coverage appears lower by QCM-D than suggested by PM-RAIRS and very close to one monolayer when compared to the theoretical coverage $\Gamma_{(th)}$.

The conclusions are thus the following: SAb is probably adsorbed in an amount close to one compact monolayer. NAV is adsorbed in a very higher amount, probably leading to compact multilayers or aggregates. Eventually, PrA does not cover the gold surface entirely and leads to a flexible layer.

Blocking Step. Figure 2Ib spectra correspond to the blocking step by BSA. One can see no significant change after contact with BSA solution for both NAV and SAb systems. For the NAV system, one even observed a small decrease of the amide bands area, likely due to the removal of some NAV molecules upon rinsing and drying. For the PrA system, the amide bands

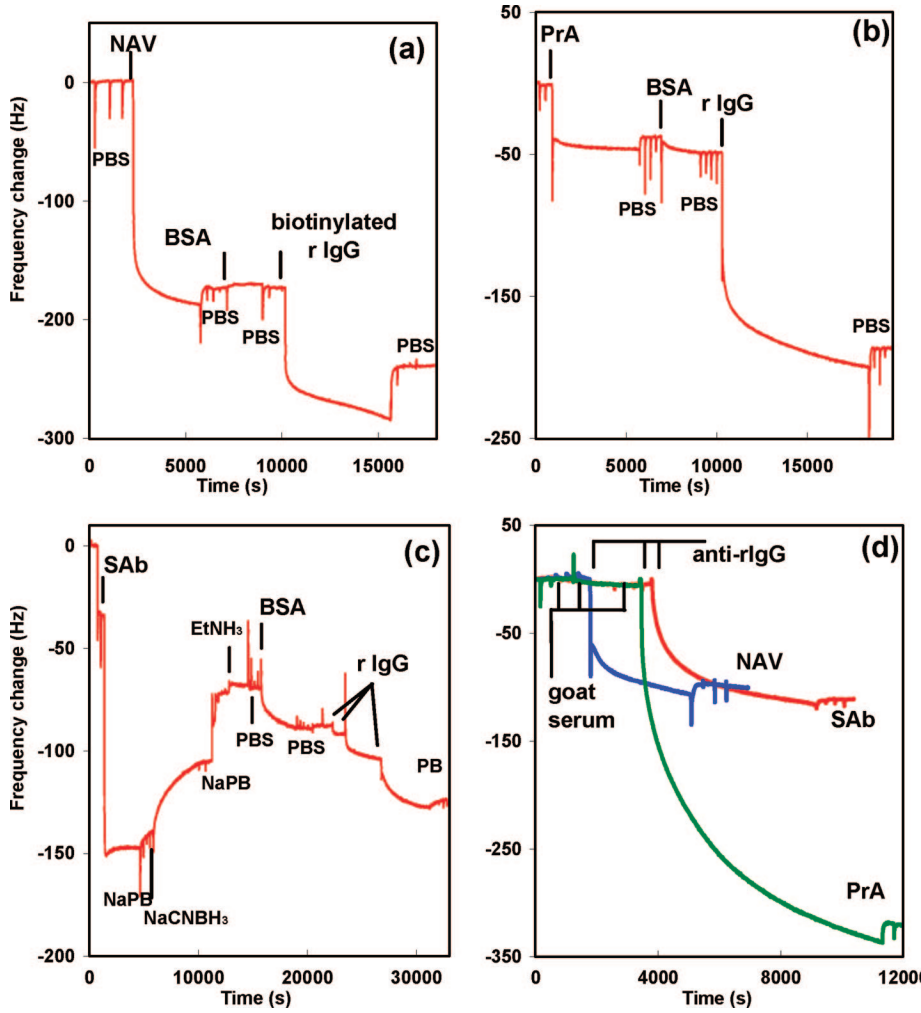

Figure 3. QCM curves for the NAV (a), PrA (b), and SAb (c) systems during immunosensors elaboration and for specificity and accessibility tests (d).

TABLE 2: QCM Results for Immunosensors Elaboration and for Accessibility Tests

system	step	ΔF (Hz)	Δm/A (ng cm^{-2})	$\Gamma_{(ex)}$ (pmol cm^{-2})	ΔD (10^{-6})	$\Delta D/\Delta F$ (10^{-6} Hz^{-1})
NAV	NAV	170	980	16.7	3	0.018
	BSA	0	0	0	−0.6	
	biotinylated rIgG	70	380	2.5	−0.2	−0.003
	antirabbit IgG	100	510	3.4	0.7	0.007
PrA	PrA	46	225	5.1	2	0.043
	BSA	10	70	1	−0.6	−0.06
	rabbit IgG	110	810	5.4	−0.4	−0.004
	antirabbit IgG	320	1988	13.2	2.6	0.008
SAb	SAb	70	405	2.7	1.2	0.017
	BSA	9	60	0.9	0.6	0.067
	rabbit IgG	40	220	1.5	1	0.025
	antirabbit IgG	110	630	4.2	4.4	0.04

area increased, as a result of BSA adsorption. This result is consistent with the previously estimated low surface coverage of PrA.

Frequency shifts measured by in situ QCM-D during the blocking step (Table 2) indicate no adsorption of BSA on the NAV-modified surface in agreement with PM-RAIRS data. Yet a small change of dissipation is recorded, which means a change in the structural properties of the layer. It is thus possible that a few NAV are exchanged by an equivalent amount of BSA, which will induce a dissipation change without a significant modification of amide band intensities. For both SAb and PrA systems, a significant decrease in frequency was recorded upon injection of BSA solution. In the case of PrA, the amount of adsorbed BSA corresponds approximately to 40% of a monolayer; which is consistent with the fraction of surface left free after the PrA adsorption Moreover, the $\Delta D/\Delta F$ ratio decreased in a considerable way, indicating a more rigid protein layer. For the SAb system, adsorption of BSA was unexpected and appears in disagreement with the PM-RAIRS results (Figure 2Ib). Moreover, this adsorption induces strong flexibility changes, as shown by the high $\Delta D/\Delta F$ ratio. Thus, the discrepancy observed between PM-RAIRS and QCM-D data may be due to the experimental conditions for SAb adsorption that involved several changes of solvent or, as suggested by the variation of dissipation, to a partial substitution of SAb by BSA that could not be detected by PM-RAIRS.

Antibody Immobilization. After this blocking step, rabbit IgG was deposited on the PrA and SAb layers. For the NAV system, we used a commercially available biotinylated rabbit IgG. PM-RAIRS spectra, recorded after the antibody adsorption step, are shown in Figure 2Ic. For the three systems, one can notice a significant increase of the amide band intensities upon antibody binding. The corresponding amide band areas, shown in Figure 2II, indicate that the amount of rIgG was the highest on the PrA layer, approximately 1.5 times higher than for the SAb system, and twice higher than for the NAV system. QCM-D data (Table 2) gave slightly different results with the PrA system being still the most efficient to immobilize rIgG followed by the NAV and SAb systems. Again, mass uptakes and experimental surface coverage values may be overestimated because of hydrodynamically coupled water. Nevertheless, as this binding step involved the same protein, we assume that the amount of hydrodynamically coupled water is the same for the three systems. Moreover, the $\Delta D/\Delta F$ ratios for NAV and PrA are very low (-0.003 and -0.004×10^{-6} Hz^{1-}, respectively) which indicates no considerable changes of the layer viscosities. The only significant change in $\Delta D/\Delta F$ ratio was recorded for the SAb system. These dissipation data allow the comparison of the QCM-D mass uptakes for the three studied systems.

The number of immobilized antibodies per capture protein, also called binding capacity, gives an idea of the efficiency of each affinity platform. Binding capacities calculated from PM-RAIRS data are equal to 0.2, 1.0, and 0.7 for the NAV, PrA, and SAb systems, respectively. QCM-D results give 0.2, 1.1, and 0.5, respectively. One observes a very good agreement between PM-RAIRS and QCM-D data for the three systems. The lowest rIgG/protein ratio was measured for the NAV platform. Actually, avidin is a tetramer with four biotin binding sites arranged in two pairs on opposed faces of the molecule.[38] Therefore, upon grafting of NAV to the biotin layer, each molecule of avidin should potentially exhibit two host sites for biotinylated rIgG. The rather low NAV binding capacity likely results from the high surface density of adsorbed neutravidin that forms multilayers or aggregates and thus leaves a limited number of accessible sites. Moreover, the NAV layer was found compact and rigid, which may decrease the accessibility of binding sites. Another possible explanation for this low binding capacity may be given by the suggested substitution of few NAV by BSA proteins. Thus, the calculated ratio Ab/NAV could be slightly under estimated. An intermediate binding capacity was measured for the SAb capture layer with a rIgG-to-SAb ratio of 0.7 (PM-RAIRS). Secondary IgG-type antibodies have two antigen-binding sites, but steric hindrance[18] may reduce the accessibility to only one of these sites; the measured ratio, 0.7, is quite reasonable and higher than that reported for similar systems without controlling the orientation of the secondary Ab.[17] This system is promising as an efficient immunosensing platform in terms of target recognition. Note that the $\Delta D/\Delta F$ ratio for SAb is the highest one at this stage, indicating a rather flexible layer. The highest antibody capacity (1.0) was measured for the PrA system. Protein A contains four high-affinity binding sites ($K_a = 10^8$ M^{-1}) capable of interacting with the Fc region of IgGs.[39,40] After immobilization of protein A on a surface, the number of available sites is lower as shown by studies on rIgG/Protein A interactions.[40–43] The binding capacity of immobilized PrA reported in the literature varies in the 0.2–0.7 range.[3,44,45] Moreover, we showed in a previous report that the binding capacity of PrA was inversely related to the surface amount of PrA.[46] The procedure described herein appears as very efficient since its both enables a high amount of rIgG molecules to be immobilized and a high binding capacity of PrA.

Specificity of the Sensing Layers and Receptor Accessibility. The specificity of the three sensing platforms was investigated using goat serum proteins as nonspecific target. As the immobilized bioreceptor was a nondirected model rIgG, we could not evaluate sensor reactivities against a specific target. Thus, we measured the accessibility of antibodies using a goat IgG anti-rIgG (anti-rIgG). The number of immobilized anti-rIgG per receptor, also called anti-rIgG-to-antibody ratio, is a good indicator of the antibody accessibility and thus of its final reactivity. Experiments were monitored by both PM-RAIRS and QCM-D.

PM-RAIRS spectra recorded, after successive exposure of the immunosensors to diluted goat serum and anti-rIgG, are shown in Figure 2Id,e. One can see that no significant change occurs after contact of any of the three immunosensors with the goat serum solution. In accordance (Figure 3d), there is no frequency change after injection of nonspecific target solution and no dissipation change; this indicates that there is no adsorption of goat serum proteins. Conversely, after interaction with anti-rIgG solution, a considerable increase of the amide bands intensities was observed (Figure 2Ie). The highest increase was observed on the PrA-mediated immunosensor, followed by the NAV and the SAb systems (Figure 2II). QCM curves are shown in Figure 3d. Again, the largest ΔF was recorded for the PrA-mediated immunosensor. For the NAV and SAb systems, the frequency variations were similar and three times smaller than for PrA. Note that at this step, reported mass uptakes may be overestimated. Actually, dissipation shifts, reported in Table 2, seem to be quite high, especially for SAb and PrA. This may indicate that QCM-D does not operate in a purely gravimetric regime any longer.[35,47] For this reason, quantitative results provided by QCM-D and PM-RAIRS (Figure 2II and Figure 3d) show some discrepancies. For the PrA and SAb systems, the amount of anti-rIgGs is almost twice higher from QCM-D than from PM-RAIRS results, when correlated to the receptor coverages. This excess demonstrates that a dissipation of about 4×10^{-6}, indicates a nongravimetrical regime for QCM. Therefore, to quantify receptors accessibility, one must focus on PM-RAIRS results, reported in Figure 2I. As shown on this figure, the anti-rIgG-to-antibody ratios are equal to 1.9, 1, and 0.7 for the NAV, PrA, and SAb systems, respectively. The highest antibody accessibility is reached for the PrA system with this immunosensor being able to capture 30 and 120% more anti-rIgG molecules than the NAV and SAb systems respectively.

Discussion

Chemisorption of NAV, PrA, and SAb to gold-coated planar IR and piezoelectric transducers yielded three different affinity platforms. Starting from similar concentrations, the amount of chemisorbed capture proteins was quite different, and the three affinity platforms displayed a variable binding capacity for rabbit IgG antibodies. This in turn had consequences on the efficiency of the antibody layers and their accessibility.

Both QCM-D and PM-RAIRS techniques suggest that only SAb molecules formed a full monolayer at the surface of the transducer, whereas PrA molecules occupied less than one monolayer and NAV amount was higher than one monolayer. One possible reason for the low amount of bound PrA is the use of glutaraldehyde as cross-linking agent; the latter may bind to the SAM amino groups via its two aldehyde terminal groups

forming bridges, thus preventing the reaction with the protein. Indeed, on a mixed SAM of 11-mercaptoundecanoic acid and 6-mercaptohexanol, where PrA was bound to carboxylic acid groups after their activation into ester functions, the recorded coverage was much higher.[48] For the SAb proteins, direct binding by reduction via their oxidized carbohydrate residues appears to be a way to reach a full coverage of the surface. On the NAV system, far from all the adsorbed NAV molecules were involved in a bioaffinity interaction with immobilized biotin. Nonspecific adsorption of NAV on the same biotinylated SAM was previously observed and assigned to the short cystamine chain.[49,50] We, however, have no clear explanation for the apparently strong binding of such a high amount of NAV. Actually, several washing steps did not remove the nonspecifically bound proteins. This nonspecific adsorption might probably be reduced by increasing the amine-terminated thiolate chain length, as described in previously cited references. Note that, in the presence of BSA, and probably due to competitive adsorption, a few NAV molecules seem to be replaced by BSA, as suggested by changes in structural properties of the adsorbed layer.

It is thus now possible to discuss the influence of the amount of adsorbed capture protein on the amount of immobilized bioreceptor, its specificity, and its accessibility. Because of the high amount of adsorbed NAV molecules, the major part of their recognition sites was not accessible; this resulted in a relatively low amount of immobilized rIgGs with a very poor antibody binding capacity of 0.2. The amount of rIgGs was slightly higher on the SAb platform with an rIgG-to-SAb ratio equal to 0.7. In a similar system, without control of secondary antibody orientation, this ratio was close to 0.3.[17] Thus, the site-selective immobilization of secondary antibody improved its binding capacity as already noticed,[6] and the objective of increasing antibody receptor density is reached. The amount of rIgGs was the highest on the PrA platform, as well as the antibody binding capacity.[1] This is likely due to the low coverage in PrA molecules that reduced steric constraints and the fact that PrA displays a high number of Fc binding sites. Interestingly, this ratio is twice higher than that measured for a similar system employing a carboxylic acid terminated SAM.[48]

The antibody binding procedure has been now well characterized; it demonstrates in particular that the density of antibody receptors on the transducer surface is markedly dependent on the affinity platform. Data concerning specificity and receptor accessibility will now be discussed. For the three elaborated antibody sensing layers, no protein was bound upon interaction with goat serum solution. Conversely, these platforms were able to specifically bind the anti-rIgG but with variable efficiencies. Despite its low surface density, or more likely thanks to it, the antibody bound to the NAV platform exhibited a good capacity to capture and bind the anti-rIgG (1.9 anti-rIgGs per rIgG). Conversely, the antibody bound to the SAb platform bound a low amount of anti-rIgGs. Finally, antibodies bound to the PrA platform had the highest anti-rIgG binding capacity, which is rather surprising as the surface coverage was also very high, close to one monolayer. If steric hindrance was the only parameter that controlled the amount of anti-rIgG bound to the antibody layer, the surface coverage in anti-rIgG should be inversely related to the surface coverage in rIgG. This is indeed the case for the SAb and NAV systems. However, for the PrA system other parameters have to be considered such as the orientation of the antibody molecules that determines which epitopes of the rIgG will be made accessible to the polyclonal goat anti-rIgG antbodies; the latter is expected to be the same as for the SAb platform. We suggest that part of the efficiency of the PrA platform arises from the flexibility as observed with the QCM-D experiments (highest $\Delta D/\Delta F$ ratio). This flexibility may be explained by the long chains used to bind PrA, and the low coverage is probably due to the cross-linker agent. The flexibility of protein layer appears to balance a high receptor coverage, thus improving binding sites accessibility. Conversely, the adsorption of NAV led to a very compact and rigid layer, which in addition to the reduced accessibility may explain the low anti-rIgG-to-rIgG ratio. In summary, the immunosensing platforms are the most efficient when one can ensure a compromise between the amount of immobilized antibodies and their accessibility. A soft and flexible layer may compensate for a reduced accessibility, increasing thus the final efficiency, as exemplified by the PrA system.

Conclusions

Comparison between immunosensors built from three different affinity platforms points out the dramatic influence of the protein adsorption mechanism. We identified three important parameters to be considered when building immunosensing platforms: the bioreceptor surface density, the accessibility of the antibody molecules, and eventually, the flexibility of the sensing layer. Upon immobilization of the capture proteins, the resulting layers at transducer surfaces were quite different: Protein A led to a partially covered surface, the amount of adsorbed secondary antibody was close to a monolayer, and avidin led to a dense, maybe multilayered, structure. We were able to classify the three affinity platforms with respect to their ability to capture a more or less large amount of rIgG, and we found out that the PrA platform was the most efficient. The model immunosensors were then treated with polyclonal anti-rIgG antibody to estimate their accessibility. The results point out that not only steric effects play an important role on the efficiency of the molecular recognition phenomena but also the layer flexibility.

Acknowledgment. This work was supported by the French Ministère de la Recherche, ACI "Energie et Conception Durable" 2004, Project No. ECD101.

References and Notes

(1) Luppa, P. B.; Sokoll, L. J.; Chan, D. W. *Clin. Chim. Acta* **2001**, *314*, 1.
(2) Briand, E.; Salmain, M.; Herry, J.-M.; Perrot, H.; Compere, C.; Pradier, C.-M. *Biosens. Bioelectron.* **2006**, *22*, 440.
(3) Briand, E.; Salmain, M.; Compere, C.; Pradier, C.-M. *Biosens. Bioelectron.* **2007**, *22*, 2884.
(4) Chung, J. W.; Park, J. M.; Bernhardt, R.; Pyun, J. C. *J. Biotechnol.* **2006**, *126*, 325.
(5) Sjoquist, J.; Meloun, B.; Hjelm, H. *Eur. J. Biochem.* **1972**, *29*, 572.
(6) Lu, B.; Smyth, M. R.; O'Kennedy, R. *Analyst* **1996**, *121*, 29R
(7) Babacan, S.; Pivarnik, P.; Letcher, S.; Rand, A. G. *Biosens. Bioelectron.* **2000**, *15*, 615.
(8) Dubrovsky, T.; Tronin, A.; Dubrovskaya, S.; Vakula, S.; Nicolini, C. *Sens. Actuators, B* **1995**, *B23*, 1.
(9) Grubor, N. M.; Shinar, R.; Jankowiak, R.; Porter, M. D.; Small, G. J. *Biosens. Bioelectron.* **2004**, *19*, 547.
(10) Oh, B.-K.; Kim, Y.-K.; Lee, W.; Bae, Y. M.; Lee, W. H.; Choi, J.-W. *Biosens. Bioelectron.* **2003**, *18*, 605.
(11) Cui, X.; Pei, R.; Wang, Z.; Yang, F.; Ma, Y.; Dong, S.; Yang, X. *Biosens. Bioelectron.* **2003**, *18*, 59.
(12) Pantano, P.; Kuhr, W. G. *Anal. Chem.* **1993**, *65*, 623.
(13) Vreeke, M.; Rocca, P.; Heller, A. *Anal. Chem.* **1995**, *67*, 303.
(14) Wilchek, M.; Bayer, E. A. *Anal. Biochem.* **1988**, *171*, 1.
(15) Witkowski, A.; Kindy, M. S.; Daunert, S.; Bachas, L. G. *Anal. Chem.* **1995**, *67*, 1301.
(16) Haugland, R. P.; You, W. W. *Methods Mol. Biol.* **1998**, *80*, 173.

(17) Kobayashi, M.; Sato, M.; Li, Y.; Soh, N.; Nakano, K.; Toko, K.; Miura, N.; Matsumoto, K.; Hemmi, A.; Asano, Y.; Imato, T. *Talanta* **2005**, *68*, 198.
(18) Xu, Y. F.; Velasco-Garcia, M.; Mottram, T. T. *Biosens. Bioelectron* **2005**, *20*, 2061.
(19) Sauerbrey, G. *Zeitschrift fuer Physik* **1959**, *155*, 206.
(20) Loefas, S.; Johnsson, B.; Edstroem, A. N. G.s.; Hansson, A.; Lindquist, G.; Hillgren, R.-M. M.; Stigh, L *Biosens. Bioelectron.* **1995**, *10*, 813.
(21) Bantegnie, A.; Boujday, S.; Pradier, C. M. Personal communication, 2005.
(22) *The Plasma Proteins: Structure, Function and Genetic Control*; Putnam, F. W., Ed.; Academic Press: New York, 1975; Vol. 1, pp 141.
(23) Bjork, I.; Petersson, B. A.; Sjoquist, J. *Eur. J. Biochem.* **1972**, *29*, 579.
(24) Reed, R. G.; Putnam, F. W.; Peters, T., Jr. *Biochem. J.* **1980**, *191*, 867.
(25) Buijs, J.; Lichtenbelt, J. W. T.; Norde, W.; Lyklema, J. *Colloids Surf., B* **1995**, *5*, 11.
(26) Caruso, F.; Rodda, E.; Furlong, D. N. *J. Colloid Interface Sci.* **1996**, *178*, 104.
(27) Caruso, F.; Rodda, E.; Furlong, D. *Anal. Chem.* **1997**, *69*, 2043.
(28) Zhou, X. C.; Huang, L. Q.; Li, S. F. Y. *Biosens. Bioelectron.* **2001**, *16*, 85.
(29) Gerdon, A. E.; Wright, D. W.; Cliffel, D. E. *Anal. Chem.* **2005**, *77*, 304.
(30) Michalzik, M.; Wendler, J.; Rabe, J.; Buttgenbach, S.; Bilitewski, U. *Sens. Actuators, B* **2005**, *105*, 508.
(31) Green, N. M. *Adv. Protein Chem.* **1975**, *29*, 85.
(32) Galli Marxer, C.; Collaud Coen, M.; Schlapbach, L. *J. Colloid Interface Sci.* **2003**, *261*, 291.
(33) Hook, F.; Kasemo, B.; Nylander, T.; Fant, C.; Sott, K.; Elwing, H. *Anal. Chem.* **2001**, *73*, 5796.
(34) Hook, F.; Voros, J.; Rodahl, M.; Kurrat, R.; Boni, P.; Ramsden, J. J.; Textor, M.; Spencer, N. D.; Tengvall, P.; Gold, J.; Kasemo, B. *Colloids Surf., B* **2002**, *24*, 155.
(35) Viitala, T.; Hautala, J. T.; Vuorinen, J.; Wiedmer, S. K. *Langmuir* **2007**, *23*, 609.
(36) Patel, A. R.; Frank, C. W. *Langmuir* **2006**, *22*, 7587.
(37) Ayela, C.; Roquet, F.; Valera, L.; Granier, C.; Nicu, L.; Pugniere, M. *Biosens. Bioelectron.* **2007**, *22*, 3113.
(38) Green, N. M. *Methods Enzymol.* **1990**, *184*, 51.
(39) Gore, M. G.; Popplewell, A. G.; Ferris, W. F.; Scawen, M.; Atkinson, T. *Biochem. Soc. Trans.* **1992**, *20*, 289S
(40) Schwartz, M. P.; Alvarez, S. D.; Sailor, M. J. *Anal. Chem.* **2007**, *79*, 327.
(41) Touhami, A.; Jericho, M. H.; Beveridge, T. J. *Langmuir* **2007**, *23*, 2755.
(42) Ahmed, S. R.; Lutes, A. T.; Barbari, T. A. *J. Membr. Sci.* **2006**, *282*, 311.
(43) Johnson, C. P.; Jensen, I. E.; Prakasam, A.; Vijayendran, R.; Leckband, D. *Bioconjugate Chem.* **2003**, *14*, 974.
(44) Pribyl, J.; Hepel, M.; Halamek, J.; Skladal, P. *Sens. Actuators, B* **2003**, *91*, 333.
(45) Atashbar, M. Z.; Bejcek, B.; Vijh, A.; Singamaneni, S. *Sens. Actuators, B* **2005**, *107*, 945.
(46) Briand, E.; Gu, C.; Boujday, S.; Salmain, M.; Herry, J.-M.; Pradier, C. M. *Surf. Sci.* **2007**, *601*, 3850.
(47) Lucklum, R. *Analyst* **2005**, *130*, 1465.
(48) Briand, E.; Salmain, M.; Compere, C.; Pradier, C.-M. *Colloids Surf., B* **2006**, *53*, 215.
(49) Pradier, C.-M.; Salmain, M.; Zheng, L.; Jaouen, G. *Surf. Sci.* **2002**, *502–503*, 193.
(50) Pradier, C. M.; Salmain, M.; Liu, Z.; Methivier, C. *Surf. Interface Anal.* **2002**, *34*, 67.

JP711916G